Application of Embedded Fiber Bragg Grating (FBG) Sensors in Monitoring Health to 3D Printing Structures

Liang Fang, Tao Chen, Ruiya Li, and Shihua Liu

Abstract—The 3D printing technology is known as a core technology in the third industrial revolution. The 3D printing structures are more popular and used as key components of products, so that monitoring health of 3D printing structures is particularly important. Moreover, the fiber Bragg grating (FBG) sensing technology is a new type of sensing technology, and FBG sensors have its unique advantages so that they have great application prospects in monitoring health of structures. FBG sensors were embedded inside a 3D printing structure, which strain variation is monitored by the FBG sensors during the loading process in this paper. Comparison was carried out between the measured and theoretical results to investigate thoroughly validity and reliability of the embedded FBG sensors for monitoring health of the 3D printing structure. Test results show that the embedded FBG sensors may be utilized to effectively monitor the strain variation of the 3D printing structure during the loading process; the measured and theoretical results show a good agreement and the straightness may be up to above 0.9998, so that the reliability is very good. Our results can also be guidance for monitoring health of 3D print structures.

Index Terms—3D printing structure, fiber Bragg grating (FBG), strain, monitoring health.

I. INTRODUCTION

THE 3D printing technology different from the traditional processing technology is an advanced and rapidly developing manufacturing technology and known as the core technology of the third industrial revolution [1]. The traditional processing and manufacturing technology generally refers to raw material blanks being processed (turned, milled, drilled, ground or machined by any other method) to remove their excess parts, manufacture qualified parts and then produce final products through assembly, welding and other means. Such technology shall belong to "subtractive manufacturing". On the other hand, the 3D printing technology is to produce final products by the layer-by-layer stacking raw

materials such as metal powder and hot melt plastic material. Such technology shall belong to "additive manufacturing". Currently, the 3D printing technology is much popular in those fields such as aerospace, mould making, biomedical and building [2]–[7]. Along with continuous improvement of the application of 3D printing technology, the aspects such as internal load transfer and damage cracks (especially monitoring their health statuses) while 3D printing products being loaded become a hot research topic.

As a new type of sensing technology, the FBG sensing technology has the advantages of high sensitivity, anti-electromagnetic interference, strong stability, wavelength division multiplexing, easy installation and so on [8], [9] so that it may be much popular in those applications such as aerospace [10], [11], shipping [12], biomedical [13], bridge [14] and mechanical industry [15], [16]. In addition, because FBG sensors are with simple structure, small diameter, and good compatibility with the substrates and other advantages, they may easily embedded in 3D printing structures for monitoring their health statuses [17], [18]. And it provides possibility for performance of real-time on-line monitoring structure stress, strain, damage cracks of 3D printing intelligent structures under manufacturing or operation. At the same time, their maintenance cost is low but their masses are not increased; thus, such technology is of great significance to improve reliability of 3D printing structures and implement structure intellectualization.

Some scholars have studied the FBG sensors embedded in composite laminates, but there is few introduction and research on the FBG sensors embedded in 3D printing structures. In this paper, FBG sensors were embedded in an equal-strength cantilever to thoroughly investigate the strain variation while it was loaded; and comparison was carried out between the measured and theoretical results to verify validity and reliability of embedded FBG sensors in monitoring health of 3D printing structures. And it provides some guiding significance for realization and development of 3D printing intelligent structures.

II. EXPERIMENTAL METHODS

A. Principle of FBG Strain Sensors

FBG is the refractive index gratings UV exposure technique in periodic distribution, by utilizing which refractive index grating may be written in optical fiber with short laser pulse
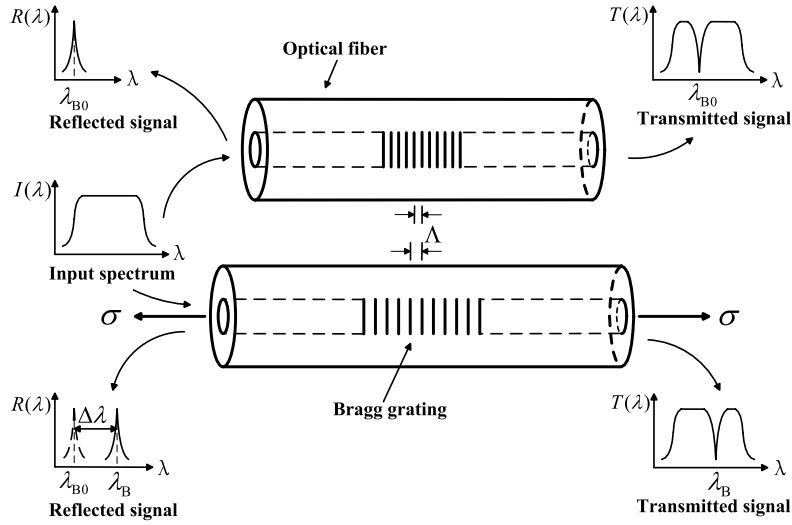
Fig. 1.   Operating principle of a FBG sensor.

interference patterns or optical fiber is annealed. When a FBG is lit with a beam of broadband light, a beam of narrow-band light with a very narrow spectrum and the center (Bragg wavelength λ) is reflected and the light with the rest wavelengths transmit the grating as shown in Fig.1 [19].

The spectra of reflection or transmission wavelengths of FBG are mainly dependent on the period and the effective refractive index of the FBG. Reflected light wavelength λ meets the Prague scattering equation, namely:

$$\lambda = 2n\Lambda \tag{1}$$

Where: λ, Λ and n present the central reflection wavelength, period and effective refractive index of the FBG, respectively.

It may be seen from Eq. (1) that the wavelength of the refractive light at the center of the FBG is directly proportional to its period and the effective refractive index of the FBG. Light whose wavelengths conform to the required conditions may be reflected by the FBG and light with other wavelengths transmit the FBG. The strain variation may directly lead to wavelength shift of the FBG, because any tension or compression of the FBG is bound to bring about changing the period of the FBG. Moreover, the FBG's photoelastic effect makes the effective refractive index n change while the external strain changes. Thus, a theoretical basis may be provided for FBG strain sensors.

When the strain is produced in the FBG, its pitch and refractive index will change accordingly; and then its corresponding wavelength shift of reflected light as shown in Fig.1 may be expressed by:

$$\Delta\lambda = \lambda_{B} - \lambda_{B0} \tag{2}$$
$$\Delta\lambda/\lambda = \Delta\Lambda/\Lambda + \Delta n/n \tag{3}$$

Where: Δn and $\Delta\Lambda$ represent the refractive index and pitch changes of the FBG, respectively.

The refractive index change of the FBG deduced by Butter and Hocker [20] first derived when any strain occurs, which may be written as:

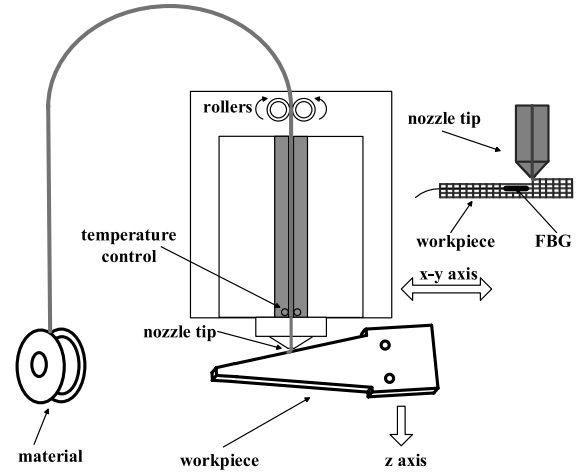$$\Delta n/n = -\frac{1}{2}n^2[(1-\mu)P_{12} - \mu P_{11}]\varepsilon = -P\varepsilon \tag{4}$$

Fig. 2.   Schematic diagram of printing a test sample.

Suppose:

$$\Delta\Lambda/\Lambda = \Delta L/L = \varepsilon \tag{5}$$

Then Eq. (3) may be converted to:

$$\Delta\lambda = \lambda(1-P)\Delta\varepsilon = k\Delta\varepsilon \tag{6}$$

Where: P represents the effective photoelastic coefficient of the FBG; for a typical quartz FBG: $n = 1.46$, $\mu = 0.16$, $P_{11} = 0.12$, $P_{12} = 0.27$ and $P = 0.22$; and $k = 0.78$ represents the sensitivity coefficient of the wavelength change due to strain.

At the same time, the temperature affect of FBG sensors may also lead to the FBG wavelength shift. Thus, temperature compensation shall be carried out by utilizing the reference FBG method in the actual measurement.

B. Manufacturing Process of 3D Printing Cantilever Structure

The FDM technology known as fused deposition modeling (FDM) technology or method is a kind of 3D printing technologies, whose schematic diagram is shown in Fig.2.
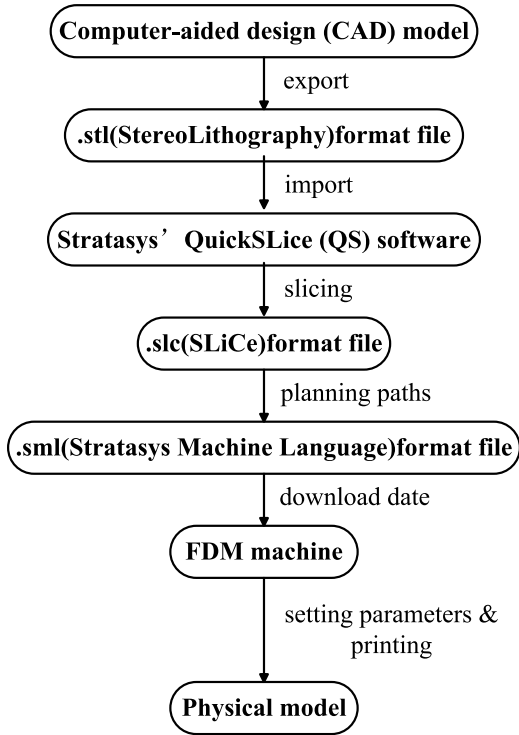
Computer-aided design (CAD) model

↓ export

.stl(StereoLithography)format file

↓ import

Stratasys' QuickSLice (QS) software

↓ slicing

.slc(SLiCe)format file

↓ planning paths

.sml(Stratasys Machine Language)format file

↓ download date

FDM machine

↓ setting parameters & printing

Physical model

Fig. 3. Flow diagram of basic FDM processes.

TABLE I
PARAMETERS OF A 3D PRINTER

Parameter	Value	Parameter	Value
Height of each layer	0.15mm	Nozzle diameter	0.4mm
Speed	30mm/s	Wire diameter	1.75mm
Temperature	473K	Wire flow	100%
Packing density	100%	Cooling time	8s

A 3D solid model is discretized into thin layers (certain layer thickness) according to the geometric parameter change to obtain the section outline and filling track. The control system heats to melt the filamentous thermoplastic material and the 3D nozzle under control of the computer moves along the section outline and filling track. And then the melt material is extruded and cooled quickly to form a cross section being bonded with the surrounding material. Each layer is stacked on the previous layer (positioning and supporting the current layer). The above process is repeated to continue melting, spraying and deposition till the entire solid modeling is completed [21].

Based on the flow diagram of basic FDM processes shown in Fig.3. Firstly, the CAD data in. stl file was established in Solidworks; secondly, the CAD model will be sliced into horizontal layers and transformed into a.slc format file; thirdly, deposition path is created for each layer and transformed into a.sml format file which is delivered to FDM machine; lastly, FDM fabrication process used a filament modeling material to build actual physical pare in an additive manner layer-by-layer. Various parameters for the print track is shown in Table I. Considering the volumes of FBG sensors, it is possible to
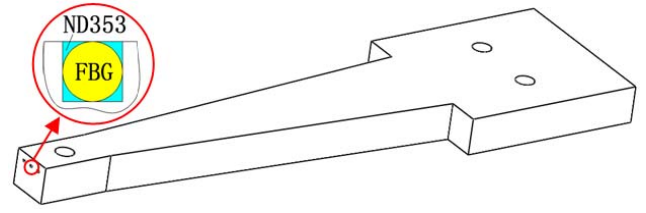

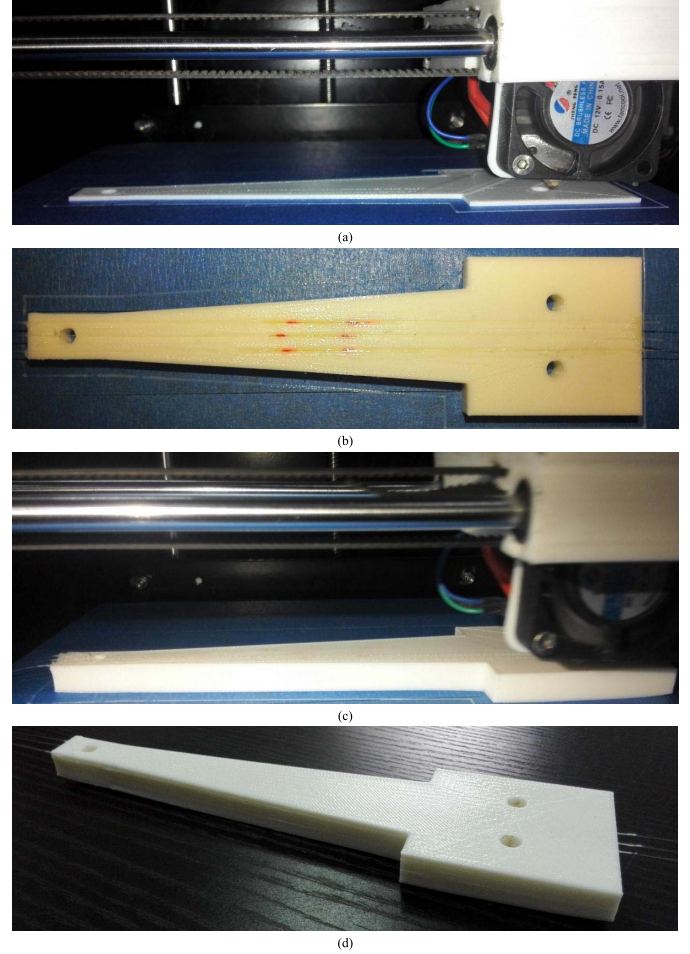Fig. 4. Structure of the cantilever.

Fig. 5. Production processes of a 3D printing test sample. (a) Lower part of the substrate of a 3D printing test sample. (b) Embedding a FBG sensor on the test substrate. (c) Upper part of the substrate of a 3D printing test sample. (d) Printing an equal strength cantilever sample.

break down the sensor while the nozzle tip is working and it also affect the quality of printing. So as shown in Fig.4, the position of the embedded sensor has a square groove.

As shown in Fig.5, firstly, the 3D printer printed out the lower part of the test sample (Fig.5.a) according to the design requirements and then FBG sensors were equipped in the square groove to continue printing and finally produce the test sample (Fig.5.c).

It is worth noting that FBG sensors shall be mounted in parallel to the cantilever during the printing process. And FBG sensors shall be free of any coating to ensure compatibility of the FBG part and the substrate. Moreover, FBG sensors was encapsulated by the glue (ND353). Furthermore, the
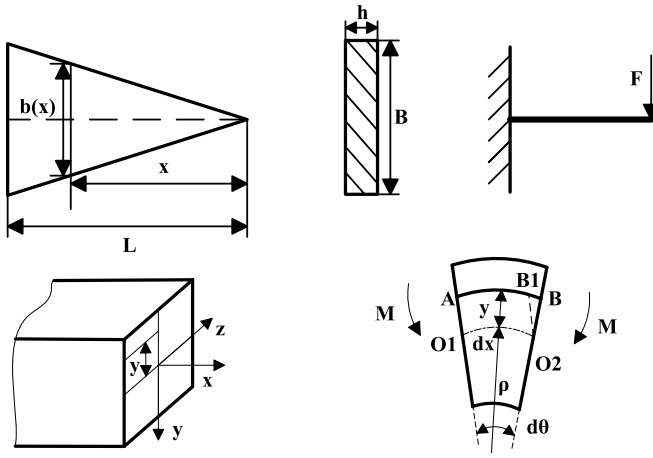
Fig. 6. Operating principle of the equal strength cantilever.

TABLE II
MECHANICAL AND GEOMETRICAL PROPERTIES OF
THE EQUAL STRENGTH CANTILEVER

Symbol	Description	Values
y	Distance from the FBG sensor to the neutral layer (mm)	3
L	Distance from Force F to the cantilever fulcrum (mm)	100
B	Large-end width of the cantilever (mm)	30
h	Thickness of the cantilever (mm)	10
E	Flexural modulus of the cantilever (MPa)[a]	2762.10

[a] Flexural modulus was tested by MTS (ceramic mechanical test system), as shown in Fig.7.

pre-stressed state shall be always maintained while FBG sensors are embedded and cured to ensure its sensing properties and precision.

C. Theoretical Calculation of Strain of Equal Strength Cantilever

Cantilevers are one of the three basic forms of statically determinate beams in engineering applications. An equal strength cantilever means that its strength is equal in each section. As shown in Fig.6, a coordinate system (X Axis: the equal strength beam center line; Y Axis: the symmetry axis of the cross section; Z Axis: the neutral axis; and the origin: the intersection point of Force F and X Axis). The bending section coefficient of the equal strength cantilever section is given as:

$$W(x) = \frac{h^2}{6}b(x) \tag{7}$$

The bending moment in the cross section of X under Force F is written as:

$$M(x) = Fx \tag{8}$$

Then, the maximum stress on the cross section becomes:

$$\sigma_{\max}(x) = \frac{M(x)}{W(x)} = \frac{6Fx}{b(x)h^2} \tag{9}$$

According to Hooke's law

$$\sigma = E\varepsilon, \tag{10}$$

then the strain is expressed as:

$$\varepsilon_{\max}(x) = \frac{6Fx}{b(x)h^2E} \tag{11}$$

Due to the thickness h of the cantilever and the expression

$$\frac{x}{b(x)} = \frac{1}{2}\cot\alpha = \frac{L}{B} \tag{12}$$

being constant and in view of a given Force F, the stress on the surface of the cantilever is maximum, which is expressed by:

$$\varepsilon_s = \frac{6FL}{Bh^2E} \tag{13}$$

As for a bending cantilever, adjacent cross sections rotate with respect to the center axis and the longitudinal linear strain of the location (y from the neutral axis) of the cross section is:

$$\varepsilon_y = \frac{\Delta\widehat{AB_1}}{\widehat{AB_1}} = \frac{\widehat{B_1B}}{\widehat{O_1O_2}} = \frac{yd\theta}{dx} \tag{14}$$

As for a bending cantilever, the length of a longitudinal line in the neutral layer is constant; and then:

$$\widehat{O_1O_2} = dx \tag{15}$$

The curvature of the neutral layer is written as:

$$\frac{1}{\rho} = \frac{d\theta}{dx} \tag{16}$$

By substituting Eq. (16) into Eq. (14), the longitudinal linear strain is derived as:

$$\varepsilon_y = \frac{y}{\rho} \tag{17}$$

Eq. (17) shows that the longitudinal line strain at any location of the cross section is proportional to the distance y from the point to the neutral axis, thus:

$$\varepsilon_y = \frac{2y}{h}\varepsilon_s = \frac{12yFL}{Bh^3E} \tag{18}$$

Various parameters of the equal strength cantilever are shown in Table 2. These parameter values are substituted into Eq. (18), and the relationship between the theoretical strain at the location of the sensor and Force F can be obtained:

$$\varepsilon_y = 43.4452F. \tag{19}$$

D. Tests of the Equal Strength Cantilever

For study of the effectiveness and reliability of FBG sensors embedded in the 3D printing structure, a test platform was established, whose schematic diagram is shown in Fig.8.

FBG sensors (wave band: 1540~1561nm) embedded in the 3D printing cantilever and a FBG demodulator (manufacturer: Wuhan WUTOS Co. Ltd.; wave band: 1525~1565nm; sampling rate: 4kHz; and wavelength resolution: 1pm) were used. Moreover, a HLA Test Stand (manufacturer:
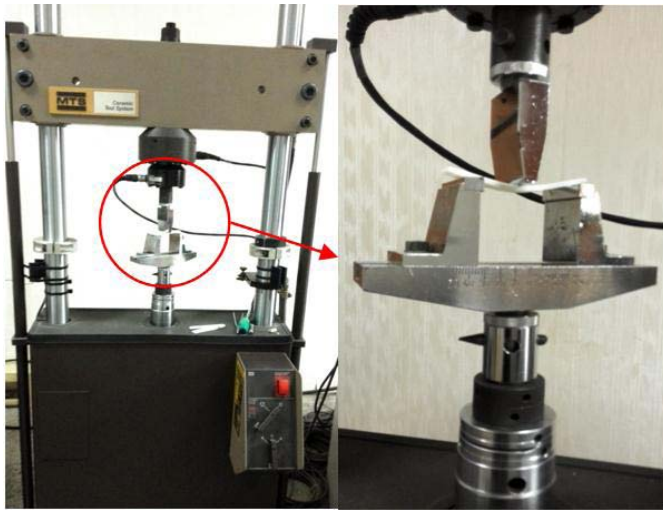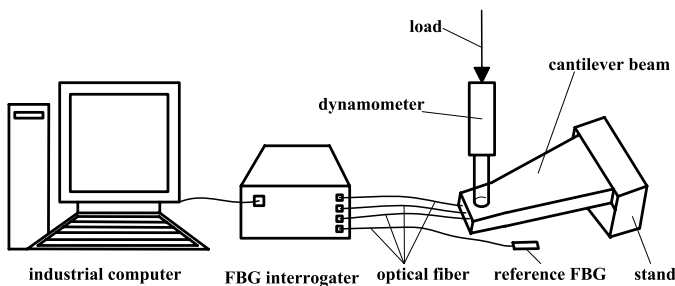
Fig. 7. MTS (ceramic mechanical test system).

Fig. 8. Schematic diagram of the test platform.

Fig. 9. Loading/unloading test.

Fig. 10. Reflected singal of the FBG sensors.

HANDPI) and a HP-50 Force Gauge (manufacturer: HANDPI; maximum load: 50N; resolution: 0.01N; and accuracy: ±0.5%) were used.

The specific test processes are as follows: the equal strength cantilever was preloaded in the test platform and the probe of the dynamometer was in alignment with the loading hole of the cantilever, and it must be ensured that the cantilever should be horizontal and the probe should be vertical because their perpendicularity may directly influence the measurement accuracy. The cantilever was loaded to the corresponding steady states (increasing and decreasing load step by step (no load – full load, namely 0-30N, increment: 2.5N/time), respectively) by rotating the hand wheel, then the corresponding readings were recorded in the dynamometer and the wavelength at the reflective center of the FBG. Such tests were carried out for 3-5 times. The loading/unloading operation is shown in Fig.9.

III. RESULTS AND DISCUSSION

A. Test Data Analysis

During the 3D printing process, reflecting wavelength of FBG sensors changed and this phenomenon testified the thermal effects and residual stress or internal stress exists in 3D printing process as shown in Fig.10. According to the principle of FBG sensors, initial reflecting wavelength does not influence the final results.

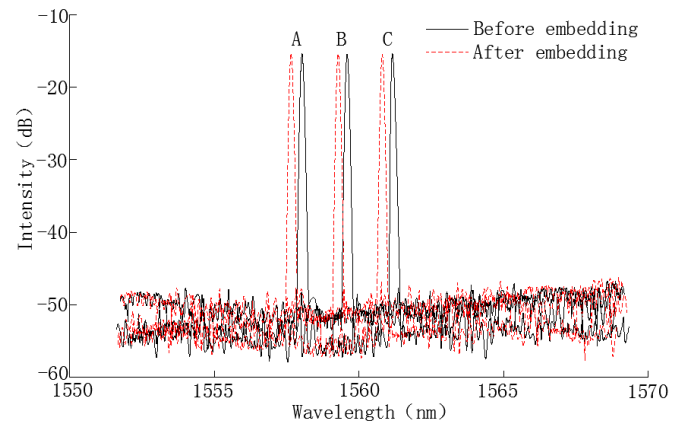The above tests were repeated for three times (16 sampling points for each time) and the corresponding FBG wavelengths were recorded under 16 groups of different loads, which were fitted and analyzed together with their corresponding wavelengths to obtain the relationship (load vs. wavelength change). The FBG sensors were labeled as FBG Sensors A, B and C, respectively.

First of all, test data were fitted by utilizing the interpolation method to loads and corresponding wavelength changes for FBG Sensors A, B and C to obtain their fitting curves and equations. At the same time, the theoretical calculation equations were converted into curves (the corresponding comparison charts are shown in Fig.11; and fitted lines and sampling points of test data for the first time are marked with A1, B1 and C1, respectively). Comparison of the fitted and theoretical results may reflect a good linear relationship (strain of FBG sensors vs. applied load; and linearity: more than 0.9999) and they are basically in good agreement. Thus, the embedded FBG sensors may be utilized to monitor any strain change inside the test sample.

Then, those measured data for three times were fitted by utilizing the interpolation method to loads and corresponding changes of wavelength of FBG Sensors A, B and C. The results are shown in Fig.12(A1, B1 and C1 refer to lines and sampling points for the first time; A2, B2 and C2 refer to lines and sampling points for the second time; and A3, B3 and C3 refer to lines and sampling points for the third time),
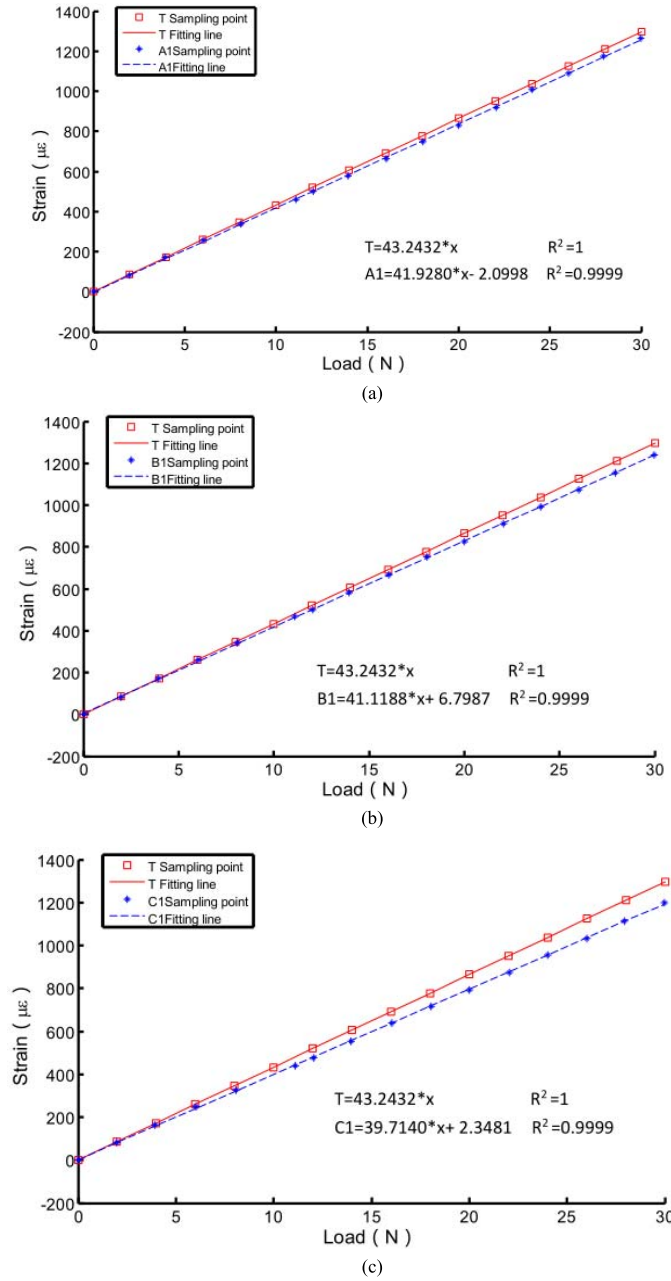
Fig. 11. Fitting curves and equations of measured and theoretical results. (a) Comparison of measured and theoretical results (FBG Sensor A1). (b) Comparison of measured and theoretical results (FBG Sensor B1). (c) Comparison of measured and theoretical results (FBG Sensor C1).
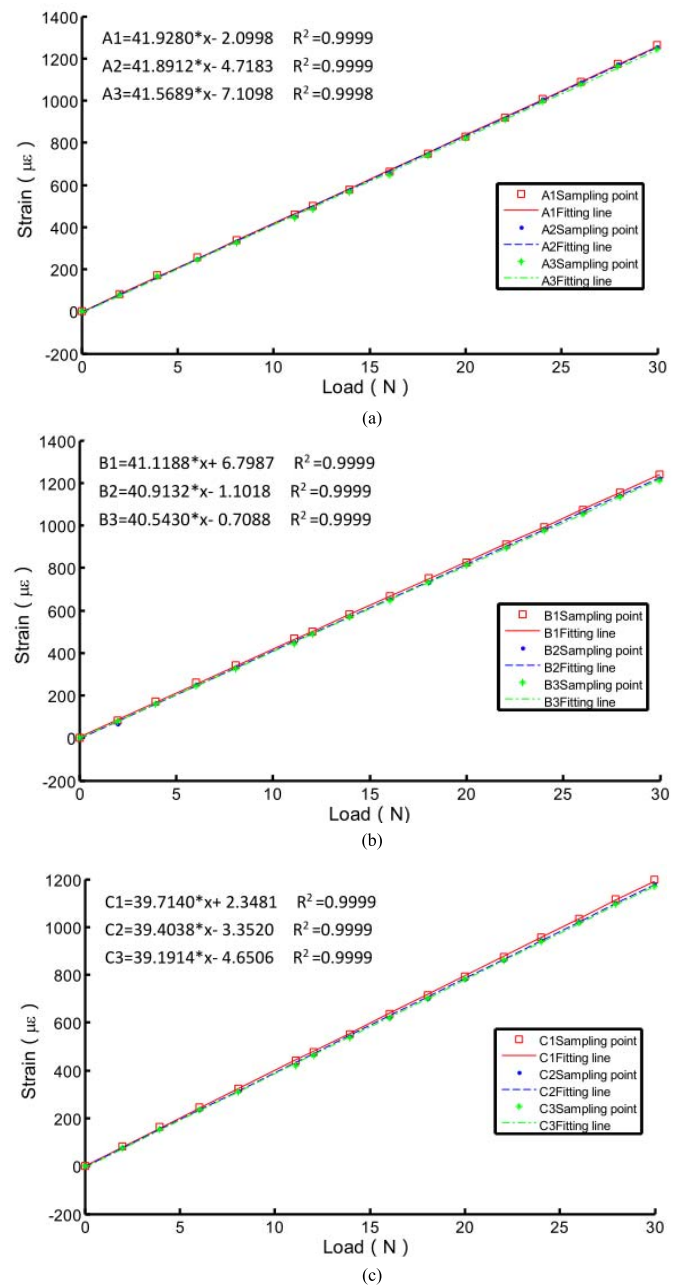

Fig. 12. Fitting curves and equations of measured and theoretical results. (a) Measured and theoretical results (FBG Sensors A1, A2 and A3). (b) Measured and theoretical results (FBG Sensors B1, B2 and B3). (c) Measured and theoretical results (FBG Sensors C1, C2 and C3).

from which it indicates that their repeatability is good and the change trends are consistent.

B. Test Error Analysis

The test errors may come from the following several aspects and the corresponding methods may be taken to further improve the measurement accuracy.

1) Loading error: loading by rotating the hand wheel, and the accuracy and the reading error of the force gauge may directly influence measurement results.
   Improvements: taking automatic loading machine and more precise dynamometer.

2) Wavelength error: measurement results may be directly influenced by the accuracy of the FBG demodulator.
   Improvements: using high-qualified FBG sensors and demodulator.

3) Test sample error: The printing layer direction and speed may affect the internal structure of the sample so that the modulus of elasticity of the sample may be influenced.
   Improvements: the rational parameters should be selected to ensure the quality of the 3D printing cantilever.

4) Cross-sensitive temperature and strain error: the elastic modulus and Poisson's ratio of the material are constant

and the cross-sensitive temperature and strain error is relatively small while the temperature change range is small.

Improvements: taking reference FBG method can eliminate the error.

5) Other errors: they (such as the strain from the cantilever to FBG sensors) are neglected due to their small influence.

IV. CONCLUSIONS

FBG sensors embedded inside a 3D printing structure were used to investigate thoroughly their validity and reliability for monitoring health of the 3D printing structure. The principle of FBG strain sensors were analyzed theoretically and test verification was carried out. The theoretical and test results are in good agreement. 3D printing structures will be much popular in various fields along with the rapid development of the 3D printing industry. It is confirmed that FBG sensors embedded inside a 3D printing structure may be utilized to accurately and effectively measure its internal strain. Our study can also be guidance for monitoring health of 3D print structures.

REFERENCES

[1] B. Berman, "3-D printing: The new industrial revolution," *Bus. Horizons*, vol. 55, no. 2, pp. 155–162, 2012.
[2] Y. Kok, X. Tan, S. B. Tor, and C. K. Chua, "Fabrication and microstructural characterisation of additive manufactured Ti-6Al-4V parts by electron beam melting," *Virtual Phys. Prototyping*, vol. 10, no. 1, pp. 13–21, 2015.
[3] J. C. Lindegaard *et al.*, "Individualised 3D printed vaginal template for MRI guided brachytherapy in locally advanced cervical cancer," *Radiotherapy Oncol.*, vol. 118, no. 1, pp. 173–175, 2015.
[4] F. Qiao *et al.*, "Application of 3D printed customized external fixator in fracture reduction," *Injury, Int. J. Care Injured*, vol. 46, no. 6, pp. 1150–1155, 2015.
[5] H. H. Malik *et al.*, "Three-dimensional printing in surgery: A review of current surgical applications," *J. Surgical Res.*, vol. 199, no. 1, pp. 512–522, 2015.
[6] L. Ding, R. Wei, and H. Che, "Development of a bim-based automated construction system," *Procedia Eng.*, vol. 85, pp. 123–131, 2014.
[7] F. C. Godoi, S. Prakash, and B. R. Bhandari, "3D printing technologies applied for food design: Status and prospects," *J. Food Eng.*, vol. 179, pp. 44–54, Jun. 2016.
[8] Y. Yang, V. G. M. Annamdas, C. Wang, and Y. Zhou, "Application of multiplexed FBG and PZT impedance sensors for health monitoring of rocks," *Sensors*, vol. 8, no. 1, pp. 271–289, 2008.
[9] X. Dong, H. Zhang, B. Liu, and Y. Miao, "Tilted fiber Bragg gratings: Principle and sensing applications," *Photon. Sensors*, vol. 1, no. 1, pp. 6–30, 2011.
[10] R. Ramly, W. Kuntjoro, and M. K. A. Rahman, "Using embedded fiber Bragg grating (FBG) sensors in smart aircraft structure materials," *Procedia Eng.*, vol. 41, pp. 600–606, 2012.
[11] A. Papantoniou, G. Rigas, and N. D. Alexopoulos, "Assessment of the strain monitoring reliability of fiber Bragg grating sensor (FBGS) in advanced composite structures," *Compos. Struct.*, vol. 93, no. 9, pp. 2163–2172, 2011.
[12] W. Shen, R. Yan, L. Xu, G. Tang, and X. Chen, "Application study on fbg sensor applied to hull structural health monitoring," *Optik-Int. J. Light Electron Opt.*, vol. 126, no. 17, pp. 1499–1504, 2015.
[13] A. Bimis, D. Karalekas, N. Bouropoulos, D. Mouzakis, and S. Zaoutsos, "Monitoring of hardening and hygroscopic induced strains in a calcium phosphate bone cement using FBG sensor," *J. Mech. Behavior Biomed. Mater.*, vol. 60, pp. 195–202, Jul. 2016.
[14] U. M. Deza, "Development, evaluation and implementation of sensor techniques for bridges critical to the national transportation system," Ph.D. dissertation, Gradworks Inc, Regina, SK, Canada, 2011.
[15] Z. Zhou, Q. Liu, Q. Ai, and C. Xu, "Intelligent monitoring and diagnosis for modern mechanical equipment based on the integration of embedded technology and FBGS technology," *Measurement*, vol. 44, no. 9, pp. 1499–1511, 2011.
[16] T. Li, Y. Tan, L. Wei, Z. Zhou, K. Zheng, and Y. Guo, "A non-contact fiber Bragg grating vibration sensor," *Rev. Sci. Instrum.*, vol. 85, no. 1, p. 015002, 2014.
[17] M. Malekzadeh, M. Gul, and F. N. Catbas, "Use of FBG sensors to detect damage from large amount of dynamic measurements," in *Proc. 30th IMAC, Conf. Struct. Dyn.*, Jacksonville, FL, USA, Jan. 30–Feb. 2, 2012, pp. 273–281.
[18] L. Ren, Z.-G. Jia, H.-N. Li, and G. Song, "Design and experimental study on FBG hoop-strain sensor in pipeline monitoring," *Opt. Fiber Technol.*, vol. 20, no. 1, pp. 15–23, 2014.
[19] K.-T. Lau, L.-M. Zhou, and J.-S. Wu, "Investigation on strengthening and strain sensing techniques for concrete structures using FRP composites and FBG sensors," *Mater. Struct.*, vol. 4, no. 1, pp. 42–50, 2001.
[20] C. D. Butter and G. B. Hocker, "Fiber optics strain gauge," *Appl. Opt.*, vol. 17, no. 18, pp. 2867–2869, 1978.
[21] I. Zein, D. W. Hutmacher, K. C. Tan, and S. H. Teoh, "Fused deposition modeling of novel scaffold architectures for tissue engineering applications," *Biomaterials*, vol. 23, no. 4, pp. 1169–1185, 2002.

Liang Fang was born in Xiangyang, China, in 1990. He is currently pursuing the Ph.D. degree with the School of Mechanical and Electronic Engineering, Wuhan University of Technology. His research fields of interest include FBG and manufacturing.

Tao Chen is currently a Professor with the School of Mechanical and Electronic Engineering, Wuhan University of Technology. His research fields of interest include digital manufacturing, design, and FBG.

Ruiya Li is currently pursuing the Ph.D. degree with the School of Mechanical and Electronic Engineering, Wuhan University of Technology. His research fields of interest include FBG and digital manufacturing.

Shihua Liu is currently pursuing the Ph.D. degree with the School of Mechanical and Electronic Engineering, Wuhan University of Technology. His research fields of interest include FBG and digital manufacturing.